Research Paper

Positional finite element solutions for laminated composites

Amal Sinaceur [a],*, Ahmed Sahli [a,b], Sara Sahli [c]

[a] *Laboratoire de recherche des technologies industrielles, Université Ibn Khaldoun de Tiaret, Département de Génie Mécanique, BP 78, Route de Zaroura, 14000 Tiaret, Algeria*

[b] *Laboratoire de Mécanique Appliquée, Université des Sciences et de la Technologie d'Oran Mohamed-Boudiaf, Algeria*

[c] *Université d'Oran 2 Mohamed Ben Ahmed, Oran, Algeria*

ARTICLE INFO

ABSTRACT

This paper deals with the development a finite element of laminated planar gantry based on the positional formulation whose kinematics enables independent turns and variation of slab thickness in an extension of the Layerwise theory. The objective is to verify the results obtained with the element proposed in this work and to compare its efficiency in relation to the two-dimensional finite elements. In addition, the analyzes are performed in order to verify the consistency, the efficiency and the robustness of the formulation with respect mainly to the correct representation of the stresses distributions.

It is intended, therefore, to obtain an element capable of performing non-linear geometric analyzes in structures of plane porticoes composed of laminated composite materials with thin or thick cross-section. Thus, the results of strain distributions and stresses are expected to be more realistic along the thickness and interfaces, aiming at future modelling of the lamination failure process by delamination or sliding. The finite element proposed in this work presents a kinematics based on the Layerwise theory, but with positions intrinsically compatible by the positional mapping functions themselves. The formulation is geometric nonlinear with the possibility of large displacements and rotations and the proposed kinematics allows to represent the Zigzag effect and the transverse heterogeneity. In all examples, numerical analyzes are performed on the Ansys software using two-dimensional finite elements.

1 Introduction

According to Carrera [1], any theory for analysis of laminated composites as well as a finite element developed with this theory should consider the following complex aspects of a laminated structure: plane anisotropy of the laminate, transverse heterogeneity, Zig-Zag effect and interlaminar continuity. The anisotropy in the laminate plane arises when the physical and mechanical properties change according to the direction considered in the plane. Laminates composed of fiber composites have high strength and stiffness along the fibers, but these properties are smaller in the transverse direction, since there is

practically only the influence of the composite matrix. This leads, according to Carrera [1], to a high flexibility in the transversal direction, as much in relation to the shear as in relation to the axial tensions.

According to Jones [2] and Reddy [3], a more relevant consequence of blade plane anisotropy relates to the coupling between the normal and shear deformations which greatly increases the difficulties in the solution procedures of laminated structures. Jones [2] and Reddy [3] also report that this anisotropy can produce an additional coupling between the deformations contained in the plane and outside it, leading to the occurrence of large displacements even at low loading levels.

The transverse heterogeneity represents the change of the physical and mechanical properties along the thickness due to the different materials employed in each blade. At the interfaces, this heterogeneity produces discontinuity of the first derivative of the displacement field with respect to the coordinate z (or 3), located along the thickness of the laminate [1-4].

The hypothesis of a linear behavior for the stress-strain relationship is widely accepted and widely used in engineering, since composite materials are strongly linear away from the rupture situation, with linearity generally superior to that of metals [5]. However, when the objective of the analysis is to identify the material failure, the effects of physical non-linearity may be important for the realistic identification of this phenomenon [6].

In view of all that has been discussed, it is concluded that the analysis of laminated composites presents major challenges, since the stress distributions in the conventional formulations are discontinuous and imprecise and their improvement is essential to define efficient failure criteria related to the laminated composite structures. Therefore, it is justified to use a discrete theory for slides in addition to the consideration of non-linear effects, since the search for a numerical formulation that realistically represents the stress distributions along the thickness and at the interfaces of a laminate considers the presence of these effects.

Many formulations are developed considering a partial Layerwise expansion of the displacement field from a Layerwise cubic variation superimposed with a piecewise function. By imposing compatibility of displacements and continuity of transverse stresses on the interfaces, the number of problem variables becomes independent of the number of slides. Already cited works with these characteristics are those of [7-11]. Other works are those of di Sciuva [12, 13], which superposed a third-order Layerwise expansion with Heaviside functions, and Icardi [13], which adopted a displacement field similar to that of [13, 14] to propose a finite curvilinear element with eight nodes for laminated plate analysis.

In this work, the formulation developed follows a kinematics similar to that adopted by the Layerwise laminate theory and uses the finite element method of positional [15-19] for the analysis of laminated flat frames considering geometric non-linearity. Thus, it is expected to obtain a more realistic distribution of tensions along the thickness and at the interfaces. The physical non-linearity is not considered, being proposed as future work.

2   Formulation

The kinematics of the laminated element is similar to that of the homogeneous element [16-17] and [20] when the cross section is composed of only one layer. In the case of rolled sections, an expansion of the kinematics of the homogeneous element is carried out in such a way as to allow the layers to have the possibility of independent rotation and variation of thickness, but with compatible interface positions. This is done by assigning independent nodal generalized vectors to the section of each layer.

The positional mapping of the element in the initial and current configurations is performed from the positions of a reference line that can be located on any layer. In this way, the degrees of freedom of the element are constituted by the positions of the nodes in the reference line and by generalized vectors that define the plane of the section of each layer.

The developed element allows having different homogeneous and isotropic materials in each layer and the constitutive model used to represent the behavior of these materials is that presented in [21-22].

The Layerwise theory assumes hypotheses that allow the representation of the anisotropy in the plane of the laminate, the transverse heterogeneity, the Zigzag effect and the interlaminar continuity.

Distributions of axial stress in the longitudinal direction and mainly of axial stress and shear in the transverse direction are obtained with excellent precision. The interlaminar continuity of the transversal stresses is not guaranteed, but the discontinuity is smaller, because the transversal deformations are discontinuous due to the independent rotation of the layers.

This discontinuity of the transverse stresses can be reduced by increasing the discretization of the section, since the number of layers of the numerical model is independent of the number of layers composing the laminate. After this, the interlaminar continuity is easily recovered by calculating the mean of the stresses obtained for the layers adjacent to a given interface.

The proposed element allows the analysis of plane frames [23] consisting of thin or thick laminates, not being subject to problems of matrix malfunctioning for these types of problems. The bad conditioning arises in the modeling of thin laminates and due to the presence of thin layers, even in thick laminates. Large variations of elastic properties of the constituent materials of the layers can also lead to problems of matrix malfunction.

Thus, when two-dimensional finite elements or finite elements developed using Reddy's Layerwise theory [3] are used to analyze laminated plane frames, inaccuracies in the results for the tension distributions, especially the transverse ones, may arise, requiring an excessive refinement of the mesh of finite elements to avoid bad conditioning

2.1 2.1 Positional mapping of the initial and current settings

The mapping of the finite element of laminated plane frame is performed by interpolating the positions of nodal points located on a reference line (*LR* - in lower case) and the generalized vectors tangent to the nodal planes of each layer. With this interpolation, the positions of any point in the element can be defined.

The positional mapping is performed in such a way that the reference line can be assigned to any layer and there is no need to be located in the center of the layer. This freedom to choose the positioning of the reference line allows assigning constraint on the positions of nodes located in any point of the cross section of the element and not only in the centroid of the section as in the case of the homogeneous plane frame element.

The initial configuration and the current configuration have their positions mapped in a similar way. In the initial configuration, the location of the reference line and node positions are information provided during pre-processing. The generalized vectors are unitary, normal to the reference line and can be obtained from the tangent vector.

In the current configuration, the positions of the reference line nodes and the generalized vectors of each layer constitute the degrees of freedom of the element, the unknowns of the problem being non-linear. In Figure 1, the idea of the positional mapping for an element consisting of five layers and cubic degree for the longitudinal polynomial interpolation employed is illustrated.

To allow locating the reference line on any layer and any position within this layer, the positional mapping of a given layer in the initial and current settings depends on whether that layer coincides with the Reference Layer (LR) or whether it is above or below this. Thus, three distinct expressions for positional mapping are required.
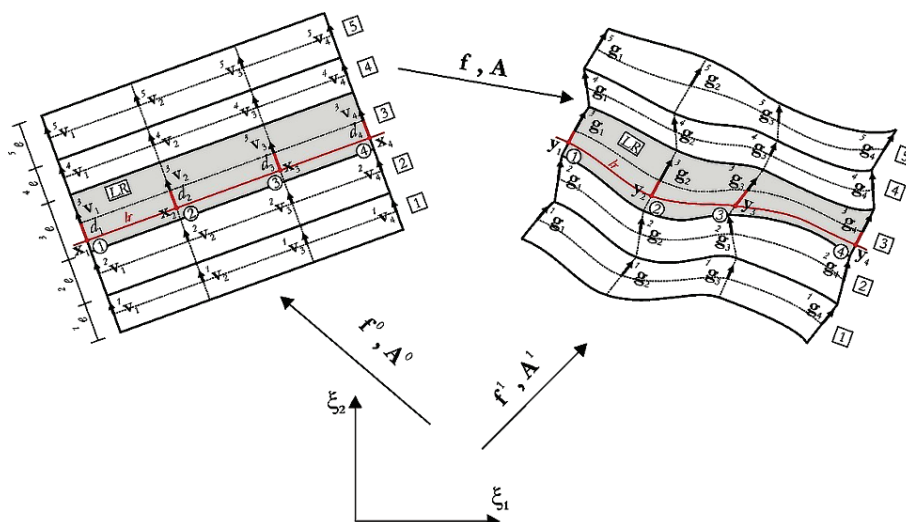

Figure 1 - Positional mapping of the laminated plane frame element

Let *k* be a map to be mapped in the initial configuration. The equations of positional mappings are expressed by:

a) Mapping for layer k equal to the Reference Layer (LR):

$$^{k}f^{0}\left(\xi_{1,}\xi_{2}\right) = {}^{k}x\left(\xi_{1,}\xi_{2}\right)$$

$$\left\{\left[d_{j}\Phi_{j}\left(\xi_{1}\right)\right] + \frac{^{k}e}{2}\xi_{2}\right\}\left[{}^{k}v_{w}^{i}\Phi_{w}\left(\xi_{1}\right)\right] \tag{1}$$

With $i = 1, 2$ and $j, w = 1, \ldots$ (gr + 1).

In this equation, $^{k}f^{0}\left(\xi_{1,}\xi_{2}\right)$ represents the positional mapping function of initial configuration $^{k}x\left(\xi_{1,}\xi_{2}\right)$ from the dimensionless space for the layer $k = LR$, $^{k}x^{i}\left(\xi_{1,}\xi_{2}\right)$ represents the initial position in the direction i of any point located in k; x_{j}^{i} is the position in the direction i of the node j located on the reference line (lr), d_{j} is the distance between the node j in the reference line and the center of the layer k, and ^{k}e is the thickness of the layer k, $^{k}v_{w}^{i}$ is the component in the i direction of the unit vector belonging to the plane of the cross section of layer k passing through the node w and $\Phi_{w}\left(\xi_{1}\right)$ is the form function associated with the node w consisting of a Lagrange polynomial with degree corresponding to the variable gr.

The vectors $^{k}v_{w}^{i}$ normal to the axis located in the center of the layers are obtained in a manner analogous to the vectors of the homogeneous plane frame element, [17].

The layers are always considered to be parallel in the initial configuration, so the vector of each layer is identical to the normal version of the reference line.

In this mapping, the first plot identifies the positions of all points belonging to the reference line and, given one point of that reference line, the second plot identifies the positions of all points in the cross section of the layer k.

When $\xi_{2} = -1$ the point is located at the lower interface of k, when $\xi_{2} = \dfrac{\left|d_{j}\Phi_{j}\left(\xi_{1}\right)\right|}{^{k}e}$ the point is located on the reference line, when $\xi_{2} = 0$ the point is located in the center of k and when $\xi_{2} = 1$ the point is located in the upper interface of k.

In Figure 2, the mapping of any point of dimensionless coordinates $\left(\xi_{1} = a, \xi_{2} = b\right)$ is illustrated.
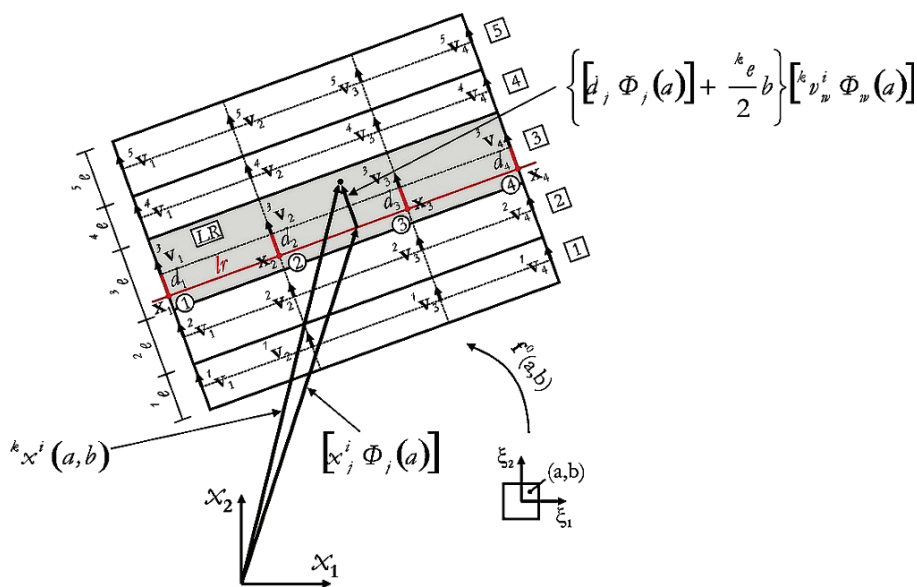

Figure 2 - Positional mapping of any point of the Reference layer in the initial configuration

b) Mapping for the layers k below the Reference Layer (LR):

$$^{k}f^{0}\left(\xi_{1},\xi_{2}\right) = {}^{k}x\left(\xi_{1},\xi_{2}\right)$$

$$^{k}x^{i}\left(\xi_{1},\xi_{2}\right) = \left[x_{j}^{i}\Phi_{j}\left(\xi_{1}\right)\right] + \left\{\left[d_{j}\Phi_{j}\left(\xi_{1}\right)\right] - \frac{^{LR}e}{2}\right\}\left[^{LR}v_{w}^{i}\Phi_{w}\left(\xi_{1}\right)\right] - \sum_{m=k+1}^{LR-1}{}^{m}e\left[{}^{m}v_{j}^{i}\Phi_{j}\left(\xi_{1}\right)\right] + {}^{k}e\left[{}^{k}v_{j}^{i}\Phi_{j}\left(\xi_{1}\right)\right]\frac{\xi_{2}-1}{2} \quad (2)$$

With $i = 1, 2$ and $j, w = 1, ..., (gr + 1)$.

In this equation, ^{LR}e and $^{LR}v_{w}^{i}$ are the thickness of the *LR* and the component in the direction i of the vector belonging to the plane of the cross section of the *LR* passing through the node *w*, respectively, and m, ^{m}e and $^{m}v_{j}^{i}$ are analogues for the layers below *LR*, ie, from layer *k + 1* to *LR - 1*. The other variables have a similar description to that of Equation (1).

In the mapping represented in equation (2), the first plot identifies the positions of all points belonging to the reference line and, given a point of that reference line, the second plot identifies the position of the point located at the lower interface of the *LR* and the third plot locates the point at the lower interface of the layer immediately above the mapped layer. Finally, the fourth plot maps all points of the cross section of layer *k*. When $\xi_{2} = -1$ the point is located at the lower interface of *k*, when $\xi_{2} = 0$ the point is located in the center of *k* and when $\xi_{2} = 1$ the point is located in the upper interface of *k*.

In Figure 3, there is an illustration of mapping any point with dimensionless coordinates $\left(\xi_{1} = a, \ \xi_{2} = b\right)$.
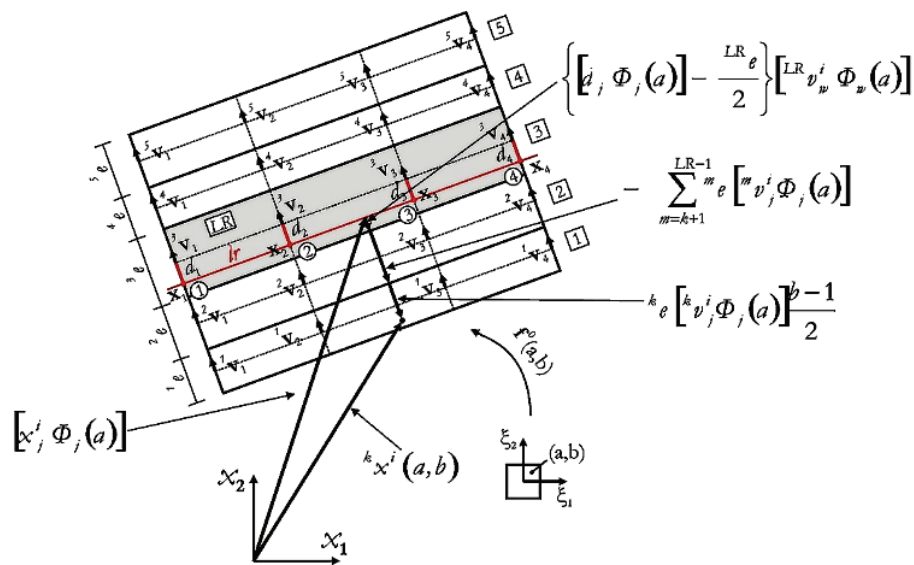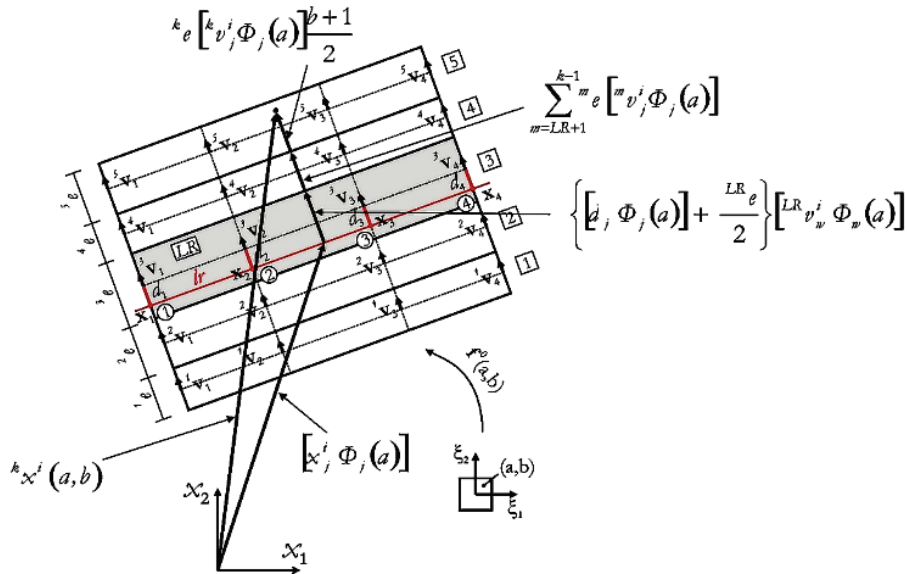

Figure 3- Positional mapping of any point in the initial configuration of a layer lower than the Reference Layer.

c) Mapping for the layers k above the Reference Layer (LR):

$$^{k}f^{0}\left(\xi_{1},\xi_{2}\right) = {}^{k}x\left(\xi_{1},\xi_{2}\right)$$

$$^{k}x^{i}\left(\xi_{1},\xi_{2}\right) = \left[x_{j}^{i}\Phi_{j}\left(\xi_{1}\right)\right] + \left\{\left[d_{j}\Phi_{j}\left(\xi_{1}\right)\right] + \frac{^{LR}e}{2}\right\}\left[^{LR}v_{w}^{i}\Phi_{w}\left(\xi_{1}\right)\right] + \sum_{m=LR+1}^{k-1}{}^{m}e\left[{}^{m}v_{j}^{i}\Phi_{j}\left(\xi_{1}\right)\right] + {}^{k}e\left[{}^{k}v_{j}^{i}\Phi_{j}\left(\xi_{1}\right)\right]\frac{\xi_{2}+1}{2} \quad (3)$$

With $i = 1, 2$ and $j, w = 1, ..., (gr + 1)$.

In this equation, and ^{m}e and $^{m}v_{j}^{i}$ are, for each layer *m* from *LR +1* to *k - 1*, the thickness and the component in the direction *i* of the vector belonging to the plane of the cross section of the layer *m* in the nodal plane *w*, respectively. The other variables have similar descriptions to the descriptions of Equations (1) and (2).

In this mapping, the first plot identifies the positions of all points belonging to the reference line and, given a point on that reference line, the second plot identifies the position of the point located at the upper interface of the *LR* and the third

plot finds the point on the interface of the layer immediately inferior to the mapped layer. Finally, the fourth plot maps all points of the cross section of layer k. When $\xi_2 = -1$ the point is located at the lower interface of k, when $\xi_2 = 0$ the point is located in the center k and when $\xi_2 = 1$ the point is located in the upper interface of k. In Figure 4, there is an illustration of the mapping of any point with dimensionless coordinates $(\xi_1 = a, \, \xi_2 = b)$.

Figure 4- Positional mapping of any point in the initial configuration of a layer above the Reference layer

The positional mapping for the current configuration is totally analogous to mapping the initial configuration by replacing the initial positions ${}^{k}x^{i}$ and x_j^i by the current positions ${}^{k}y^{i}$ and y_j^i and the vectors ${}^{LR}v_j^i$, ${}^{m}v_j^i$ and ${}^{k}v_j^i$ by the generalized vectors ${}^{LR}g_j^i$, ${}^{m}g_j^i$ and ${}^{k}g_j^i$ in all mapping expressions.

In this way, the layer mappings in the current configuration are expressed by:

a) Mapping of layer k equal to the Reference Layer (LR):

$$ {}^{k}f^1\left(\xi_{1,}\xi_2\right) = {}^{k}y\left(\xi_{1,}\xi_2\right) $$

$$ {}^{k}y^i\left(\xi_{1,}\xi_2\right) = \left[y_j^i\Phi_{\mathrm{j}}\left(\xi_1\right)\right] + \left\{\left[d_j\Phi_{\mathrm{j}}\left(\xi_1\right)\right] + \frac{{}^{k}e}{2}\xi_2\right\}\left[{}^{k}g_w^i\Phi_w\left(\xi_1\right)\right] \tag{4} $$

With i = 1, 2 and j, w = 1, …., (gr + 1).

b) Mapping of the layers k below the Reference Layer (LR):

$$ {}^{k}f^1\left(\xi_{1,}\xi_2\right) = {}^{k}y\left(\xi_{1,}\xi_2\right) $$

$$ {}^{k}y^i\left(\xi_{1,}\xi_2\right) = \left[y_j^i\Phi_{\mathrm{j}}\left(\xi_1\right)\right] + \left\{\left[d_j\Phi_{\mathrm{j}}\left(\xi_1\right)\right] - \frac{{}^{LR}e}{2}\right\}\left[{}^{LR}g_w^i\Phi_w\left(\xi_1\right)\right] - \sum_{m=k+1}^{LR-1}{}^{m}e\left[{}^{m}g_j^i\Phi_{\mathrm{j}}\left(\xi_1\right)\right] + {}^{k}e\left[{}^{k}g_j^i\Phi_{\mathrm{j}}\left(\xi_1\right)\right]\frac{\xi_2-1}{2} \tag{5} $$

With i = 1, 2 and j, w = 1, …., (gr + 1).

c) Mapping of the layers k above the Reference Layer (LR):

$$ {}^{k}f^1\left(\xi_{1,}\xi_2\right) = {}^{k}y\left(\xi_{1,}\xi_2\right) $$

$$ {}^{k}y^i\left(\xi_{1,}\xi_2\right) = \left[y_j^i\Phi_{\mathrm{j}}\left(\xi_1\right)\right] + \left\{\left[d_j\Phi_{\mathrm{j}}\left(\xi_1\right)\right] + \frac{{}^{LR}e}{2}\right\}\left[{}^{LR}g_w^i\Phi_w\left(\xi_1\right)\right] + \sum_{m=LR+1}^{k-1}{}^{m}e\left[{}^{m}g_j^i\Phi_{\mathrm{j}}\left(\xi_1\right)\right] + {}^{k}e\left[{}^{k}g_j^i\Phi_{\mathrm{j}}\left(\xi_1\right)\right]\frac{\xi_2+1}{2} \tag{6} $$

With $i = 1, 2$ and $j, w = 1, ..., (gr + 1)$.

In these expressions, the current positions of the nodes located on the reference line, represented by y_j^i, and the generalized vectors of the nodal sections of each sheet $^k g_j^i$ constitute the degrees of freedom of the finite element laminated. The element was developed in order to allow the use of any number of layers to compose the cross section and any degree to the polynomial approximation functions.

3   Numerical treatment

In all, two examples were analyzed to evaluate different aspects of the formulation. The results obtained with the finite element proposed in this work are compared to the results obtained from analytical solutions and to the results obtained through numerical analyzes with two-dimensional finite elements performed in Ansys software. In the latter case, the finite element employed was PLANE42. This is a finite two-dimensional rectangular element with four nodes that employs linear shape functions to interpolate nodal displacements.

In the analysis carried out in Ansys, a very refined discretization was employed, the results of which are used as reference for comparison. In addition, also the analyzes with discretizations equivalent to the discretizations used in the analysis made with the finite element laminated are carried out. For this, a number of PLANE42 elements equal to the number of layers were added between two nodes of the discretization with the element of laminated plane frame. This work aimed to compare the performance of the element proposed in this work in relation to two-dimensional finite elements that can present problems of matrix mismatch when used in the analysis of laminated plane frames. This may lead to the need for refinement of the two-dimensional finite element mesh and consequently to increase computational cost.

The objective with the analysis of the first four examples is to verify the different aspects of the formulation. Thus, the first example is constituted by a homogeneous biased beam subjected to the action of a uniform distributed load. In this example, the main objective is to verify the convergence of the discretization both in relation to the number of elements and in relation to the number of layers used to represent the cross section. The problem was analyzed for three situations with the relation between span and height of the beam ($S = L/h_0$) assuming the values of 2, 4 and 10. In all analysis, the displacement and stress distributions along the cross section at different points of the beam are verified.

In the second example, a biased sandwich beam with uniform distributed loading applied to the upper face is analyzed. The beam is similar to the first problem and was also analyzed for the three span and height ratios ($S = 2, 4$ and 10). The main objective with this example is to verify the accuracy of the displacement and stress distributions along the cross section for the rolled case, as well as to evaluate the efficiency of the element in problems whose S ratio varies from thin to thick. In addition, the possibility of applying distributed forces outside the reference line is verified.

Having verified the formulation in the previous examples, two frames consisting of one and five decks, with laminated sections, were proposed and analyzed. The results of the displacement distributions along the cross section of some points are presented.

As far as the literature review of this work continued, no examples of laminated plane frames were found in the literature. All the problems found were restricted to laminated beams analyzed in the linear regime. Thus, this example contributes with results that may be used in future verification of formulations that deal with the problem of geometric nonlinear analysis of laminated plane frames.

In summary, it was sought, with these analyzes, to verify the various aspects of the formulation of the laminated plane frame element in addition to evaluating its efficiency and consistency.

3.1   *Homogeneous beam biased with distributed force*

In this first example, a biased and homogeneous single beam subjected to the action of uniformly distributed loading is analyzed, as shown in Figure 5. The geometric characteristics of the cross section and the elastic parameters of the material are also represented in said figure.
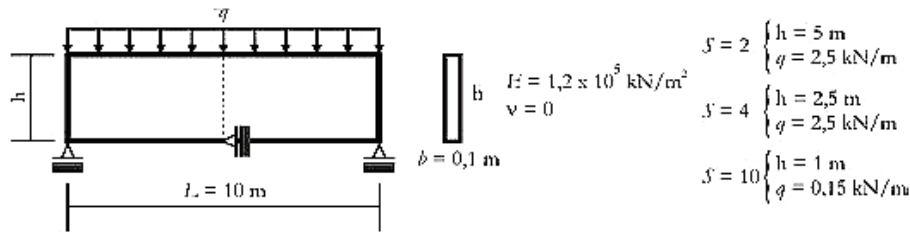
Figure 5 - Geometry, loading and elastic parameters for the problem.

In all analyzes, the distributed force was applied in a single increment, because the value of the force considered is low to maintain the problem in the regime of small deformations and to allow a comparison with the analytical solution obtained from the Classical Theory of Beams (CTB) that is based on Euler-Bernoulli's kinematic hypotheses. Moreover, a Poisson coefficient (ν) null is also adopted. It is worth mentioning that the distributed force is applied to the upper face of the beam while the reference line is located on the lower face, where the supports are.

The problem was analyzed for three situations with the relation between span and height of the beam ($S = L/h$), assuming the values of 2, 4 and 10. We sought to verify the ability of the formulation to accurately represent the displacement distributions and tensions for problems with relation between span and height corresponding to slender beams and high beams (wall beams).

In order to evaluate the convergent ability of the formulation, the beam was discretized with a number of cubic finite elements ranging from 2, 4, 8 and 16. Twenty layers were used to discretize the cross section, since this was the number of layers provided a good distribution for the transverse shear stress. This was verified for the case of the beam with $S = 10$, which was analyzed by a discretization composed by 4 finite elements and by a number of layers ranging from 1, 2, 4, 8, 20 and 40.

The solution process based on the Newton-Raphson method was controlled by means of the convergence criteria in position and force with tolerances of 10^{-9} and 10^{-6} respectively. The number of Gauss points used in the numerical integrations of the internal forces vector and the Hessian matrix was 4 x 20 (span x height) on each layer. This quantity of Gauss points was adopted after a comparative study of the values obtained for the horizontal displacement u of the lower face of the section located 2.5 m from the left support, from the vertical displacement v and of the axial tension S_{11} of the lower face of the localized section in the middle of the span of the beam. In this study, numerical integrations were performed with the number of Gauss point's variable up to a limit of 20 x 20.

This study was performed for the beam of the case $S = 10$, discretized with 4 finite elements and with a number of layers ranging from 1, 2, 3, 4, 8 and 20 layers.

From these observations, it is reasonable to assume that 4 Gauss points along the longitudinal direction is sufficient for the finite element with degree of cubic interpolation and that more Gaussian points along the transverse direction are required the larger the number of layers adopted.

The computational implementation of the formulation does not allow the adoption of different amounts of Gaussian points in each layer. Thus, it was not possible to identify if there are differences in the amount of Gauss points needed for the layers close to the Reference layer and for the layers distant from the layer.

Thus, to guarantee a correct numerical integration and since the problems presented in this work do not have a high degree of freedom, 4 x 20 Gauss points were adopted in all analyzes.

In Figure 6, the results of a convergence analysis for the case of the beam whose relationship between span and height (S) is equal to 10. The beam is discretized with 4 cubic elements and only the number of layers is varied. As can be seen, from 1 layer in the discretization of the section, the results for the displacement u and for the axial stress S_{11} already coincide with the analytical solution and with the numerical solution obtained in the Ansys from a very refined discretization. However, the shear stress S_{12} was only reasonably represented from a discretization with 8 layers. From 20 to 40 layers, the improvement in the representation of tension S_{12} occurred only in the lower and upper faces, where the values are the lowest.

As there was no significant gain in stress distributions after increasing from 20 to 40 layers, in all other analyzes performed in this example and in Examples 1.2, a discretization of the 20 layers section was adopted.

The analysis of the beams with a relationship between span and height (S) equal to 2, 4 and 10 were performed by varying only the number of finite elements (4, 8 and 16 elements). The results of the horizontal displacement distributions u, axial stress in the longitudinal direction S_{11}, axial stress in the transverse direction S_{22} and shear stress S_{12} are shown in Figure 7, Figure 8, Figure 9 and Figure 10, respectively. All the stresses represented are average between elements and the interlaminar continuity of the stresses is represented by calculating the average values obtained at the interfaces of the adjacent layers. In these figures, also the average results obtained through numerical analyzes performed in Ansys using the two-dimensional finite element PLANE42 are shown. The equivalence between the finite positional element and the PLANE42 element mesh was made so that there is a PLANE42 element between two nodes and one element on each layer. The number of degrees of freedom is also conserved. This equivalence results in the following association:

- Positional with 4 cubic elements and 20 layers $\Leftrightarrow$ PLANE42 with 12 x 20 mesh elements;

- Positional with 8 cubic elements and 20 layers $\Leftrightarrow$ PLANE42 with a mesh of 24 x 20 elements;

- Positional with 16 cubic elements and 20 layers $\Leftrightarrow$ PLANE42 with mesh of 48 x 20 elements.

The analytical results obtained from the CTB (only for the case with S = 10) and those obtained by means of analyzes in the Ansys using a very refined discretization are also presented and adopted as reference to evaluate the precision of the results obtained with the element of laminated planar frame.
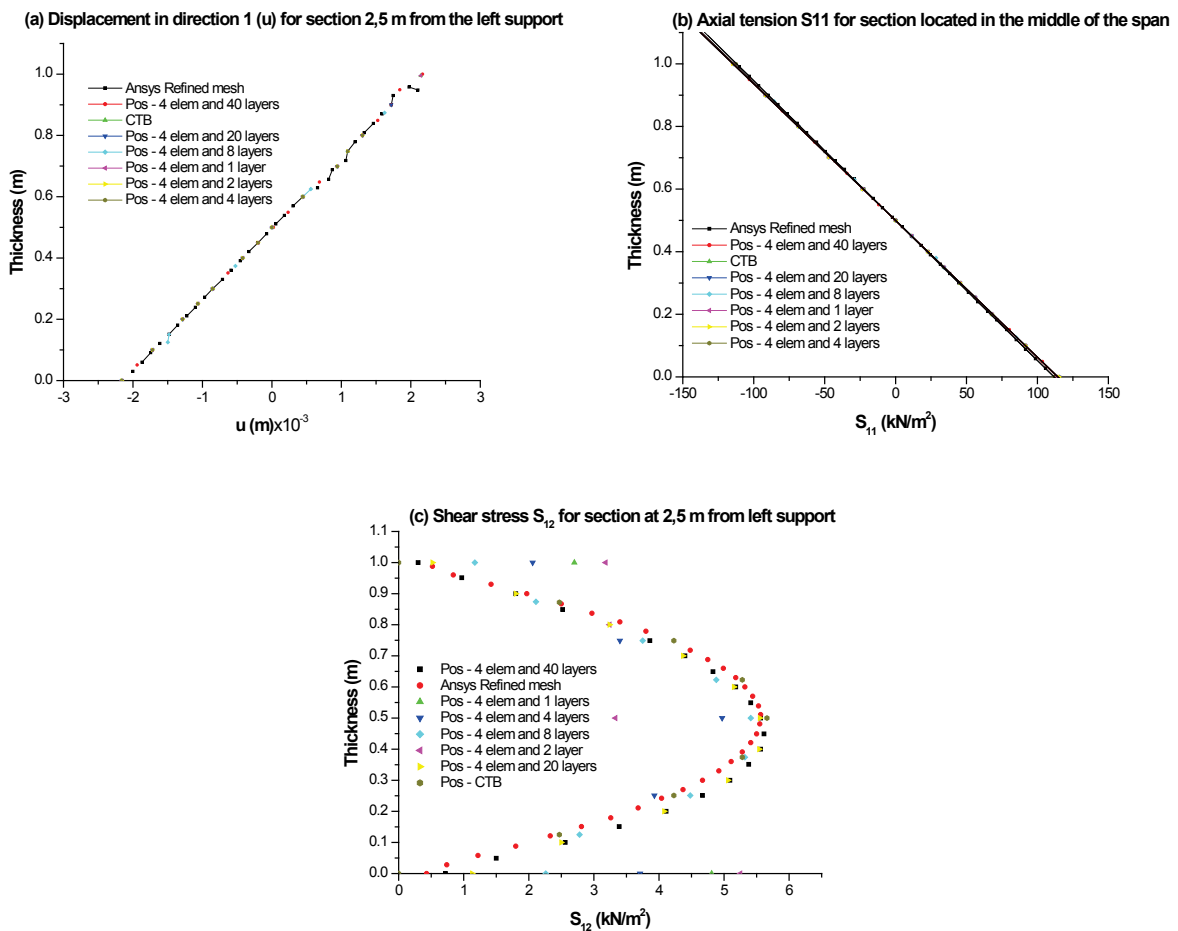

Figure 6 - discretization with 4 cubic elements and variation of the number of layers (Case with S = 10).

The displacement distributions shown in Figure 3 were correctly obtained with a discretization in 4 finite elements. The shape of the section was plotted in accordance with the results of the analytical solution based on the CTB, in the case with

S = 10, and the numerical solution obtained in the Ansys with a refined mesh. It is worth noting that the proposed finite element was able to represent the curved shape of the section for the case of the beam with S = 2.

It is also observed that the results obtained with the equivalent meshes in the Ansys show some influence of the matrix malfunction suffered by the two-dimensional finite element. For the beam with S = 10, the PLANE42 elements have greater distortion and there were differences in the displacement distribution obtained. For the beam with S = 2, the PLANE42 elements are less distorted due to the greater beam height and there are practically no differences in the displacement distribution. All these aspects mentioned above are also verified for the distribution of axial stresses S_{11} in the longitudinal direction, as can be seen in Figure 8.

As shown in Figure 9 and Figure 10, the axial strain distributions S_{22} and S_{12} shear stress required a larger discretization (8 finite elements) for an acceptable representation. However, a good agreement with the results of the analytical solution based on the CTB, in the case with S = 10 and tension S_{12}, and of the numerical solution obtained in the Ansys with a refined mesh was reached for a discretization with 16 finite elements.

Despite the requirement for a greater discretization, the results obtained in the Ansys with equivalent meshes were not better than those obtained with the laminated plane frame element. This is observed mainly for the S_{12} shear distributions in the case of the beams with S = 4 and S = 10. In these beams, the two-dimensional element PLANE42 seems to suffer from problems of matrix malfunctioning due to a greater distortion of the element generated by the equivalent discretization and by the smaller height of the beams.
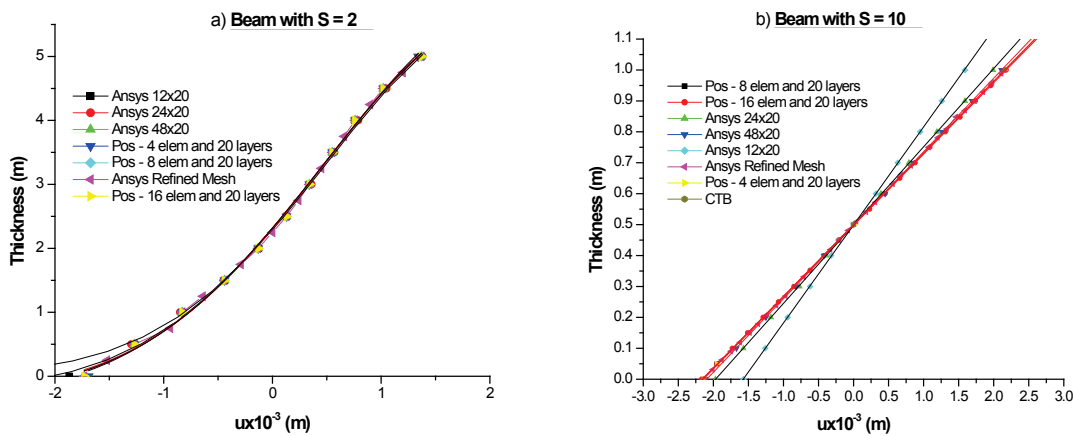

Figure 7 - Displacement in direction 1 (u) for section at 2.5 m from left support.

3.2 Biased sandwich beam with distributed force

The same beam of the previous example is analyzed, but now the section is composed of three layers forming a sandwich laminate composite. The layers of the faces have a thickness corresponding to 5% of the total height and modulus of elasticity equal to 100 times the modulus of elasticity of the layer that composes the core. The geometric characteristics of the cross section and the elastic parameters of the material are shown in Figure 11.

The problem was analyzed again for three situations with the relation between span and height of the beam ($S = L / h_0$) assuming the values of 2, 4 and 10. It was therefore sought to verify also in the case of a laminated beam the ability of the formulation to accurately represent the displacement and stress distributions in problems with different slenderness ratios. The beam was discretized with 16 finite elements and 20 layers, 4 on the lower face layer, 12 on the core layer and 4 on the upper face layer (4/12/4 notation).
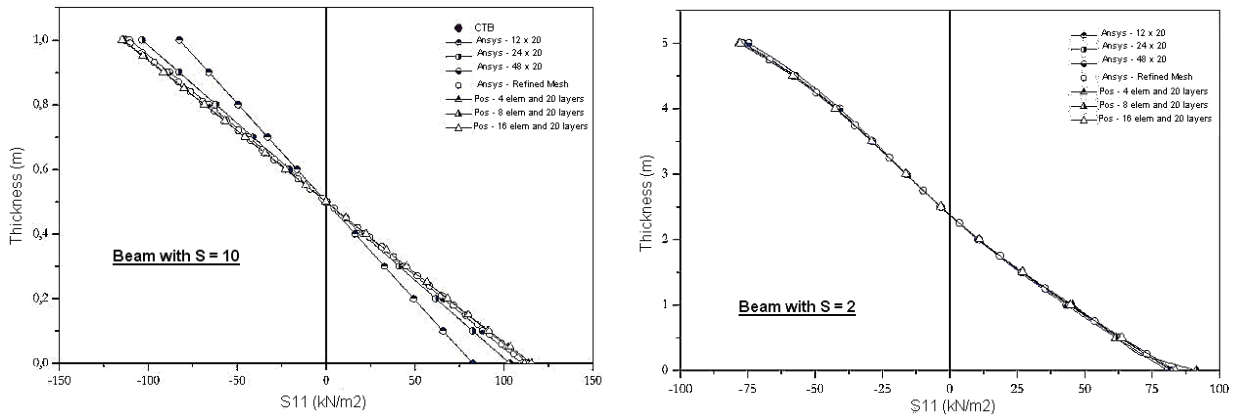
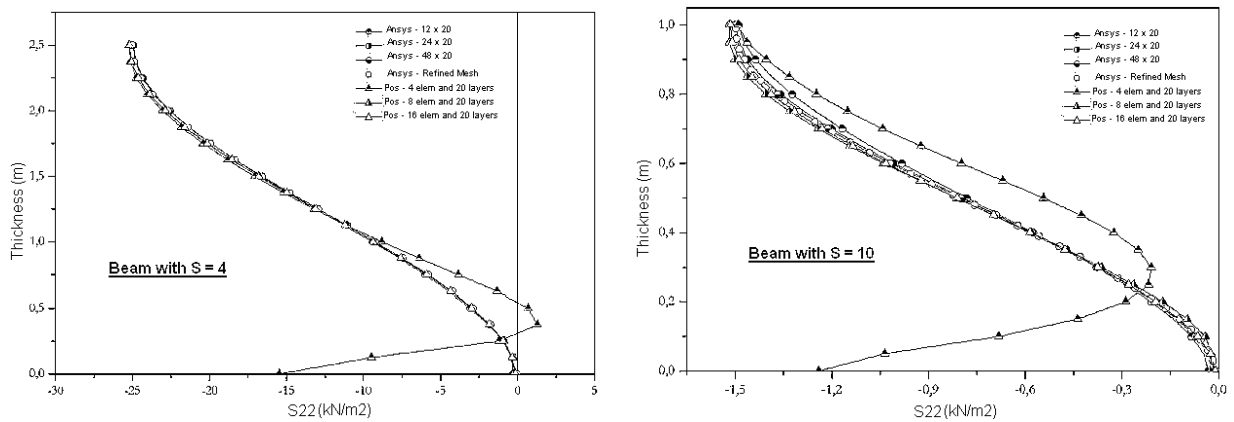*Figure 8 - Axial tension S_{11} for section located in the middle of the span.*

Figure 9 - Axial tension S_{22} for section located in the middle of the span.
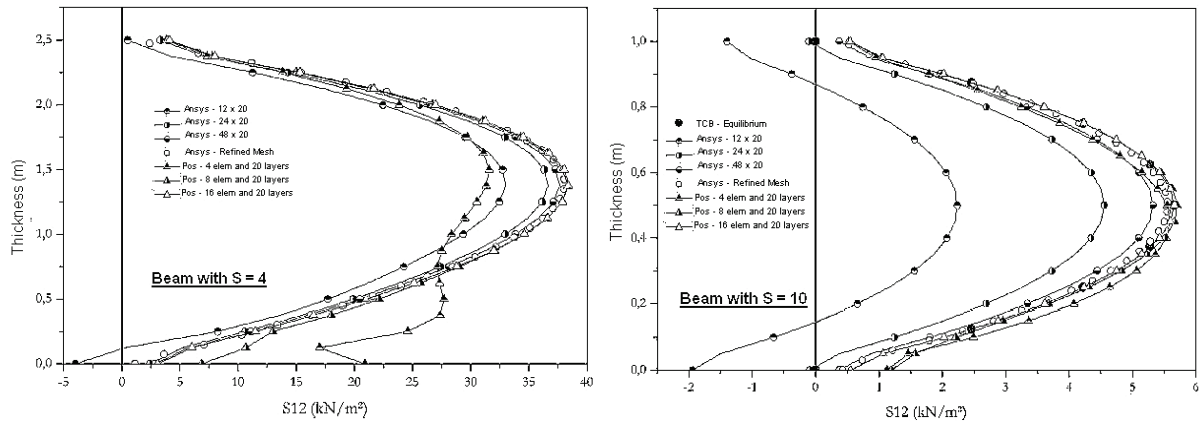

Figure 10 - Shear stress S_{12} for section at 2.5 m from left support.

This discretization was adopted based on the observations extracted from the convergence analyzes performed in the previous example.

In all analyzes, the distributed force was applied in a single increment and the solution process based on the Newton-Raphson method was controlled by means of the convergence criteria in position and force with tolerances of 10^{-9} and 10^{-6}, respectively. The number of Gauss points employed in the numerical integrations of the internal forces vector and the Hessian matrix was 4 x 20 on each discretization layer.
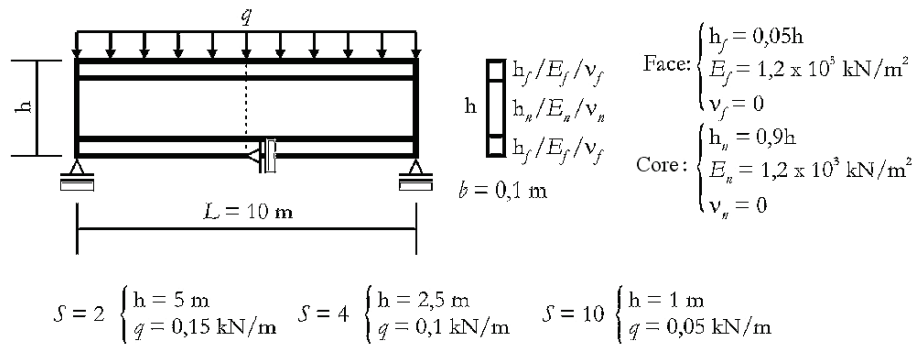
Figure 11 - Geometry, loading and elastic parameters of the problem 2.

The results of the analyze are presented through the distributions of (Fig. 12), longitudinal axial stress S_{11} (Figure 13), axial cross-stress S_{22} (Figure 14) and shear stress S_{12} (Figure 15). All stresses shown are averages between elements and the interlaminar continuity of the axial stress S_{11} between layers of the same material and the transverse stresses S_{12} and S_{22} between any layers is represented by averaging the values obtained at the interfaces of the adjacent layers.
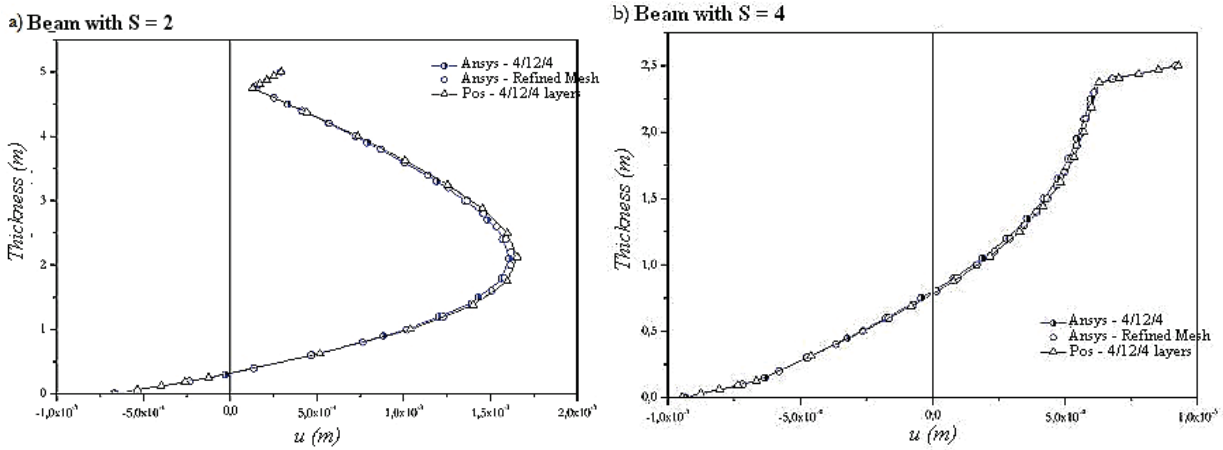

Figure 12 - Displacement in direction 1 (u) for section at 2.5 m from left support.

In these figures, also the average results obtained from numerical analyzes performed in Ansys using the two-dimensional finite element PLANE42 are shown. The equivalence between the finite positional element mesh and the PLANE42 element was done in a manner analogous to the previous example. This equivalence results in the following association:

- Positional with 16 cubic elements and 20 layers (4/12/4) $\Leftrightarrow$ PLANE42 with a mesh of 48 x 20 elements, with 20 distributed on 4/12/4.

Results obtained from numerical analyzes performed on Ansys using very refined discretization are also presented and adopted as reference.

Thus, the accuracy of the results obtained with the laminate plane frame element was excellent, since an excellent agreement with the reference results was achieved as shown in the representation of the horizontal displacement u, the longitudinal axial tension S_{11}, the transverse axial tension S_{22} and the shear stress S_{12} in Figure 12, Figure 13, Figure 14, Figure 15, respectively.

The results obtained in Ansys using the two-dimensional finite element PLANE42 through an equivalent mesh showed less precision for the tensions S_{11} and S_{12} in the region around the interfaces between the layers. This lower precision is attributed to a possible matrix malfunction caused by both the distortion of the PLANE42 element and the change in the elastic properties of the material in the interface region.

Depending on the performance achieved, the possibility of applying distributed forces outside the element reference line can be considered as consistent. All of these observations highlight the suitability and efficiency of the proposed element to analyze thin-walled (portico) or non-plane (plate) problems, consisting of laminated composites.
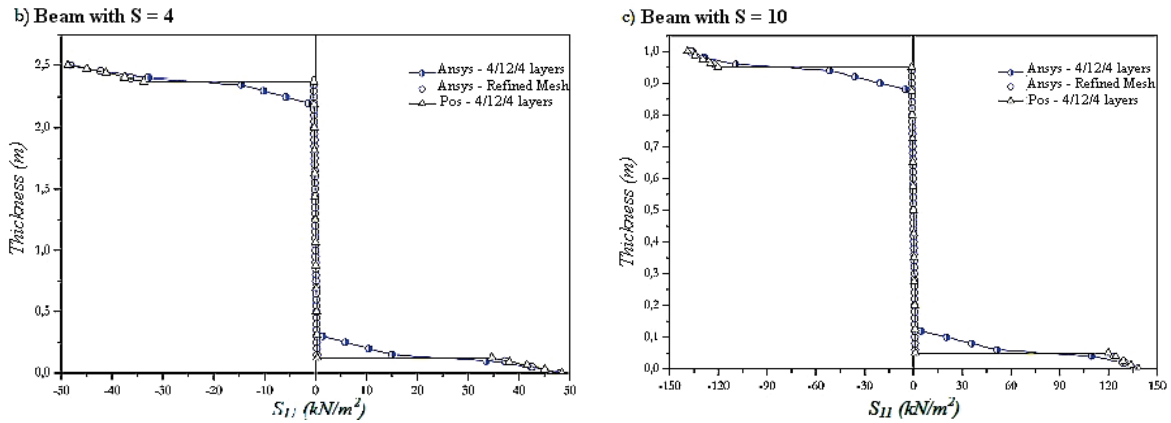
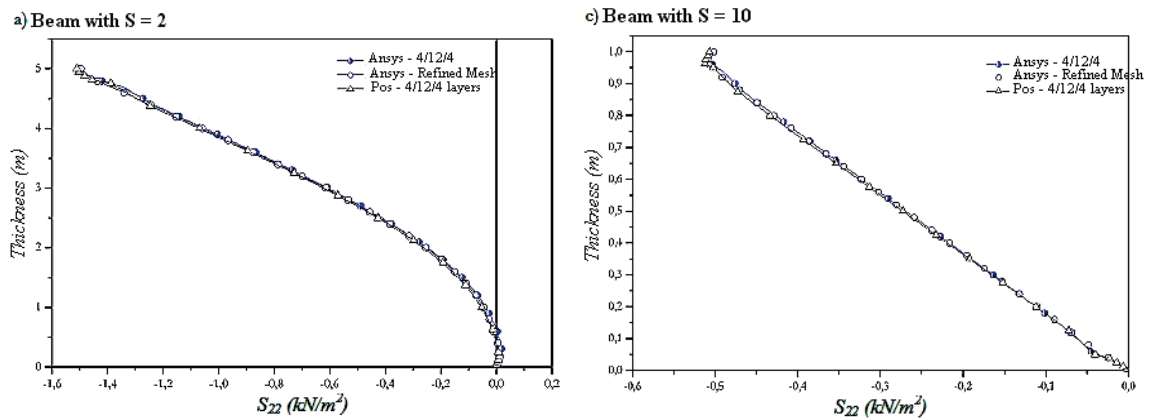*Figure 13 - Axial stress S_{11} for section located in the middle of the span.*

Figure 14 - Axial tension S_{22} for section located in the middle of the span.
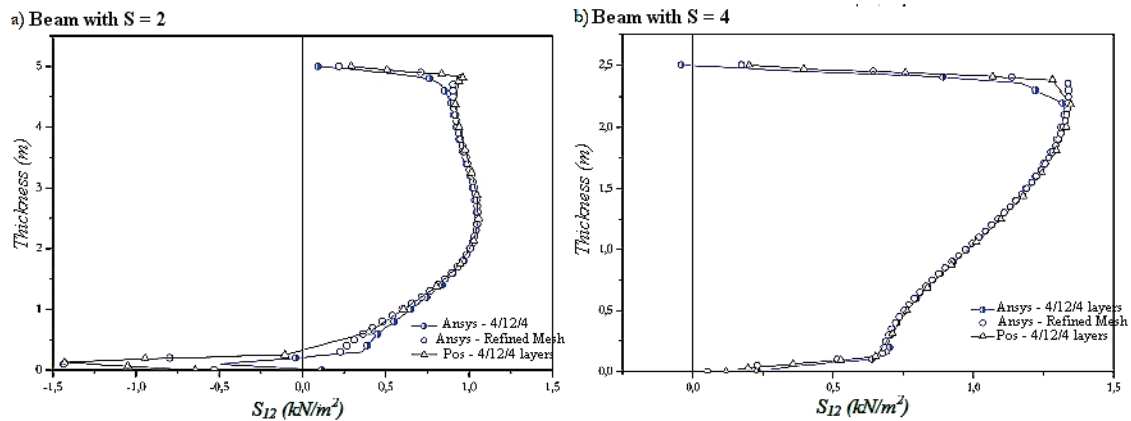

Figure 15 - Shear stress S_{12} for section at 2.5 m from left support.

The analysis of the two examples allowed evaluating several characteristics of the formulation of the laminated frame plane element. The results obtained were satisfactory and both the element formulation and its computational implementation performed in FORTRAN programming language were verified.

From the results obtained in Example 1, it was found that a finer finite element mesh is needed to obtain a suitable representation of the stress distributions along the cross section, particularly the shear stresses. Regarding the displacements, a much smaller discretization already converges to the values adopted as reference. Another important observation is that an increasing number of Gaussian points distributed along the thickness of the layers is necessary as the amount of layers used in the section discretization is increased.

In Examples 2, the possibility of applying distributed forces and concentrated forces outside the element reference line was evaluated and considered consistent since satisfactory results were obtained for the displacement and stress distributions in the cross sections. In this example, it has also been found that the use of the two-dimensional element PLANE42 in the Ansys program presents problems of matrix mismatch caused by the distortion of the elements and the abrupt variation in the elastic properties of the material from one layer to another. This fact is not observed in the laminated   plane element, demonstrating its efficiency to analyze plane problems (thin or not) made of laminated composites.

The penalization technique employed to perform coupling of elements was also efficient. Its versatility was verified in the possibility of representing connections with any rigidity. Finally, results of the displacement distributions along the cross section were presented for two proposed frame examples. Thus, a contribution is made to reduce the difficulty in finding results of nonlinear geometric analyzes in examples of laminated plane frames, glimpsing future work applications.

4   Conclusions

The formulations of two positional finite elements were developed, implemented and verified by analysis of problems with analytical and numerical solutions available in the literature or found from numerical analyzes performed in Ansys software. The first element developed was the homogeneous plane frame with degrees of freedom composed of nodal positions and by generalized vectors representing the rotation and the variation in the height of the cross section. Problems with varied characteristics of geometry, loading, contour and stiffness of the links between bars were analyzed. The results confirmed the consistency, efficiency and robustness of the element formulation, since an excellent agreement with reference results was verified. Thus, the element is suitable to carry out geometric nonlinear analysis in structural models of plane frame whose current configurations can present great displacements and rotations, but with linear elastic behavior for the material that must exhibit moderate deformations. In view of the good performance presented by the homogeneous plane frame element, a natural expansion of its kinematics was used for the development of the laminated plane frame element.

REFERENCES

[1]- E. Carrera, Theories and Finite Elements for Multilayered Anisotropic, Composite Plates and Shells. Arch. Comput. Method. E. 9(2) (2002) 87-140. doi:10.1007/BF02736649

[2]- R.M. Jones, Mechanics of composite materials. 2nd Ed. New York: Taylor & Francis, 1998.

[3]- J.N. Reddy, Mechanics of laminated composite plates and shells: theory and analysis. 2nd Ed. CRC Press, 2003.

[4]- Q. Zhao, C.C. Qian, L.T. Harper, N.A. Warrior, Finite element study of the microdroplet test for interfacial shear strength: Effects of geometric parameters for a carbon fibre/epoxy system. J. Compos. Mater. 52(16) (2018) 2163-2177. doi:10.1177/0021998317740943

[5]- P.T.R. Mendonça, Composite materials and sandwich structures: design and analysis. (in Portuguese). Ed. Manole, 2005.

[6]- K.N. Spanos, N.K. Anifantis, Mechanical characterization of hexagonal boron nitride nano composites: A multiscale finite element prediction. J. Compos. Mater. 52(16) (2018) 2229-2241. doi:10.1177/0021998317740942

[7]- J.G. Ren, A new theory of laminated plate. Compos. Sci. Technol. 26(3) (1986) 225-239. doi:10.1016/0266-3538(86)90087-4

[8]- J.G. Ren, Bending theory of laminated plate. Compos. Sci. Technol. 27(3) (1986) 225-248. doi:10.1016/0266-3538(86)90033-3

[9]- J.G. Ren, Bending of simply-supported, antisymmetrically laminated rectangular plate under transverse loading. Compos. Sci. Technol. 28(3) (1987) 231-243. doi:10.1016/0266-3538(87)90004-2

[10]- A. Toledano, H. Murakami, A high order laminated plate theory with improved in plane responses. Int. J. Solid. Struct. 23(1) (1987) 111-131. doi:10.1016/0020-7683(87) 90034-5

[11]- D. Li, X. Li, J. Dai, Process Modelling of Curing Process-Induced Internal Stress and Deformation of Composite Laminate Structure with Elastic and Viscoelastic Models. Appl. Compos. Mater. 25(3) (2018) 527-544. doi:10.1007/s10443-017-9633-5

[12]- M.D. di Sciuva, Bending, vibration and buckling of simply supported thick multilayered orthotropic plates: An evaluation of a new displacement model. J. Sound Vib. 105(3) (1986) 425-442. doi:10.1016/0022-460X(86)90169-0

[13]- M. Cho, R.R. Parmerter, An efficient higher-order plate theory for laminated composites. Compos. Struct. 20(2) (1992) 113-123. doi:10.1016/0263-8223(92)90067-M.

[14]- U. Icardi, Eight-noded zig-zag element for deflection and stress analysis of plates with general lay-up. Compos. Part B-Eng. 29(4) (1998) 425-441. doi:10.1016/S1359-8368(97)00040-1.

[15]- H.B. Coda, R.R. Paccola, An alternative positional FEM formulation for geometrically non-linear analysis of shells: curved triangular isoparametric elements. Comput. Mech. 40(1) (2007) 185-200. doi:10.1007/s00466-006-0094-1

[16]- H.B. Coda, A solid-like FEM for geometrically non-linear 3D frames. Comput. Method. Appl. Mech. E. 198(47-48) (2009) 3712-3722. doi:10.1016/j.cma.2009.08.001

[17]- H.B. Coda, R.R. Paccola, A FEM procedure based on positions and unconstrained vectors applied to non-linear dynamic of 3D frames. Finite Elem. Anal. Des. 47(4) (2011) 319-333. doi:10.1016/j.finel.2010.11.001

[18]- J.P. Pascon, H.B. Coda, Large deformation analysis of elastoplastic homogeneous materials via high order tetrahedral finite elements. Finite Elem. Anal. Des. 76 (2013) 21-38. doi:10.1016/j.finel.2013.08.006

[19]- M.S.M. Sampaio, Non-linear geometric analysis of fiber-reinforced laminated shells. Thesis (Doctoral Degree in Structural Engineering) - Department of Structural Engineering, School of Engineering of São Carlos, University of São Paulo, São Carlos, 2014.

[20]- H.B. Coda, R.R. Paccola, Improved finite element for 3D laminate frame analysis including warping for any cross-section. Appl. Math. Model. 34(4) (2010) 1107-1137. doi:10.1016/j.apm.2009.07.020

[21]- M.A. Crisfield, Non-linear Finite Element Analysis of Solids and Structures, Volume 1, essentials. John Wiley & Sons, 1991.

[22]- J.N. Reddy, An Introduction to Nonlinear Finite Element Analysis: with applications to heat transfer, fluid mechanics, and solid mechanics. Oxford University Press, 2014.

[23]- L.F. Martha, Analysis of structures: Basic concepts and methods. (in Portuguese) Ed. Elsevier Brasil, 2010.